2014 IEEE Military Communications Conference

Designing Radio Interferometric Positioning Systems with Undersampling Techniques

Marie Shinotsuka*, Yiyin Wang†, Xiaoli Ma*, and G. Tong Zhou*
*School of Electrical and Computer Engineering, Georgia Institute of Technology, Atlanta, Georgia 30332–0250
†Department of Automation, Shanghai Jiao Tong University, Shanghai, 200240, China

***Abstract*—The associated location information is crucial for the data collected by wireless sensor newtworks (WSNs), and nodes have to locate themselves when they are deployed randomly. The radio interferometric positioning system (RIPS) provides high accuracy at low-complexity, which is suitable for cost-limited nodes in WSNs. In the RIPS, two transmitters transmit sinusoids at slightly different frequencies, and the received signal is squared to achieve a low-frequency differential signal at the receivers. The phase difference of the low-frequency differential signals at two receivers is estimated to achieve a range metric called the Q-range, which is a linear combination of distances among four nodes. The squaring operation, however, increases the noise power that degrades the range-estimation performance, and also the Q-range estimator with the traditional RIPS receivers consists of the approximation error. To overcome these drawbacks, we propose the RIPS receiver employing the undersampling techniques (RIPS-u) that directly samples the received signal. By avoiding the squaring operation, the RIPS-u can achieve high accuracy and obtain the Q-range estimate without approximation. We provide the MATLAB simulation results to confirm the effectiveness of our proposed RIPS-u.**

I. Introduction

As the technology advances, cost and size of the hardware decrease, which allows wireless sensor networks (WSNs) to be used in a wide range of applications including environmental monitoring, target tracking, and navigation [1]. In many of these applications, node locations are crucial since sensor data such as temperature and humidity becomes meaningless without the location of where that data is obtained [2] [3].

The localization algorithms can be classified into two general categories: range-free and range-based localization. The range-free localization algorithms are generally low-complexity but can only provide coarse accuracy [4]–[7]. On the other hand, the range-based schemes can achieve higher accuracy by calculating the position from estimated ranges. Timestamps are employed to estimate the time-of-flight (TOF) in [8], [9]. The use of the ultra-wideband (UWB) short pulses [10] and acoustic signals [11], [12] are also proposed, although high sampling rate in the UWB short pulses is often too demanding for typical low-cost devices in WSNs, and acoustic interference is still a challenge for sound signals.

Y. Wang was supported by the National Nature Science Foundation of China (No. 61301223) and the Nature Science Foundation of Shanghai (No. 13ZR1421800).

The radio interferometric positioning system (RIPS) was first proposed in [13] as an accurate localization system with low-complexity for WSNs, and it estimates the range based on the signal phase. In the RIPS, two nodes transmit pure sinusoids at slightly different frequencies. These transmitted sinusoids interfere, which yields a low-frequency differential signal. A linear combination of distances between nodes called the Q-range is obtained from the phase difference of the received differential signals at two receivers. Since the frequency of the differential signal is designed to be small, only low sampling rate is necessary at the receivers. With commercially available RF devices, the field experiment presented in [13] achieves a submeter accuracy.

Because of its low complexity and high accuracy, the RIPS has been enhanced in various directions. In [14] and [15], the RIPS has been implemented in the 2.4 GHz range. The spinning beacons are used in [16], where beacons are spinning while transmitting the sinusoids. Thus, the Doppler frequency is measured to estimate the angle-of-arrival (AoA). Tracking of the mobile node is another application that the RIPS can be employed [17], [18]. The asynchronous RIPS (ARIPS) [19] uses a dual-tone signal to deal with the clock uncertainties between nodes, and the RIPS under multipath environment is considered in [20]. These are examples of different improvements made on the RIPS, and they show the flexibility of the RIPS.

One of the advantages of the RIPS is that the sampling rate can be low since the receiver samples the low-frequency differential signal, which is extracted by a square-law device. Squaring the signal, however, increases its noise power, which degrades the range-estimation performance. To avoid the increase in the noise power, we propose the RIPS receiver that directly samples the downconverted signal and achieves a linear combination of distances without approximation. We show that the phase can be accurately estimated even if frequencies are aliased due to undersampling since the signals used in the RIPS are narrowband. Hence, the parameter design is more flexible using our proposing RIPS receiver compared to the traditional RIPS receiver. For the rest of this paper, we denote our proposing system as the RIPS-u and the conventional RIPS receiver with square-law devices as the RIPS-sq.

In summary, the advantages of the proposed RIPS-u over the RIPS-sq are as follows: 1) the noise power is lower, 2) the Q-range can be estimated without approximation, and 3) parameter design is more flexible. The performance of the

978-1-4799-6770-4/14 $31.00 © 2014 IEEE
DOI 10.1109/MILCOM.2014.56

RIPS-u and the RIPS-sq are evaluated through simulations, and the results confirm that the RIPS-u achieves high accuracy.

The rest of this paper is organized as follows. Section II describes the system model of the RIPS-u and the RIPS-sq. In Section III, the Q-range estimator is presented for the RIPS-u. The MATLAB simulation results are shown in Section IV, and the paper concludes in Section V.

II. System model

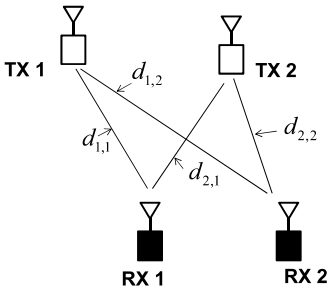

Fig. 1. The radio interferometric ranging technique.

Let us recall the ranging procedure in the RIPS [13]. Each ranging session in the RIPS involves four nodes (two transmitters and two receivers) as illustrated in Fig. 1. Here, only the receivers are assumed to be perfectly synchronized, and transmitters can be asynchronous in time. At each ranging session, two transmitters transmit at slightly different frequencies. The bandpass complex representation of the transmitted signal at the kth transmitter node is given as

$$s_k(t) = a_k e^{j2\pi\theta_k} e^{j2\pi f_k t},\ k = 1, 2 \tag{1}$$

where $a_k e^{j2\pi\theta_k}$ and f_k are the complex amplitude and the frequency of the signal transmitted by the kth node, respectively. Without loss of generality, let us assume $f_1 > f_2$ and define $\delta = f_1 - f_2$ and $g = (f_1 + f_2)/2$. Frequencies are designed such that $\delta \ll f_1, f_2$, and hence $f_1, f_2 \approx g$.

When the signals arrive at the receiver, they are delayed by the propagation time proportional to the distance that they travel. Then, the signal is downconverted to the intermediate frequencies by the local oscillator at the frequency f_o. Assuming the channel between the transmitter and the receiver only contains the additive white Gaussian noise (AWGN), the downconverted received signal at the lth receiver is modeled as

$$\begin{aligned} r_l(t) =& a_1 e^{j2\pi(f_1 - f_o)t} e^{-j2\pi\varphi_{1,l}} \\ &+ a_2 e^{j2\pi(f_2 - f_o)t} e^{-j2\pi\varphi_{2,l}} + v_l(t), \end{aligned} \tag{2}$$

where $\varphi_{k,l} = f_k(d_{k,l}/c + t_k) - \theta_k$ is the phase of the received signal from the kth transmitter to the lth receiver, $d_{k,l}$ is the distance between the kth transmitter and the lth receiver, c denotes the speed of light ($c = 3 \times 10^8$), t_k is the unknown time instant when the kth node starts its transmission, and $v_l(t)$ is the AWGN with the variance σ_l^2. Note that t_k is unknown due to the lack of synchronization between the transmitter and the receiver. In the following subsections, we first review the received signal model in the RIPS-sq, followed by the signal model in our proposing RIPS-u.

A. The RIPS-sq

The receiver block diagram of the RIPS-sq is shown at the lower part of Fig. 2. In the RIPS-sq, the downconverted received signal $r_l(t)$ is passed through a band-pass filter (BPF) and a square-law device to obtain a low-frequency differential signal component in the analog domain. A low-pass filter (LPF) is further applied to remove high frequency components and any noise outside of the band of interest. Multiplying the received signal $r_l(t)$ with its complex conjugate and removing the DC and high frequency components, the resulting low-frequency differential signal is

$$\begin{aligned} \tilde{r}_l(t) =& a_1 a_2 e^{j2\pi\delta t} e^{-j2\pi\phi_l} + a_1 a_2 e^{-j2\pi\delta t} e^{j2\pi\phi_l} + \tilde{v}_l(t), \end{aligned} \tag{3}$$

where $\phi_l = \varphi_{1,l} - \varphi_{2,l} = f_1(d_{1,l}/c + t_1) - \theta_1 - f_2(d_{2,l}/c + t_2) + \theta_2$, and $\tilde{v}_l(t)$ is the aggregated noise term containing all the terms related to $v_l(t)$. Then, the low-frequency differential signal $\tilde{r}_l(t)$ is sampled at the rate f_s, where $f_s \geq 2\delta$. Collecting N samples, we achieve

$$\tilde{\mathbf{r}}_l = \tilde{\mathbf{H}}\tilde{\mathbf{z}}_l + \tilde{\mathbf{v}}_l, \tag{4}$$

where $\tilde{\mathbf{r}}_l$ and $\tilde{\mathbf{v}}_l$ are sampled vector of $\tilde{r}_l(t)$ and $\tilde{v}_l(t)$, respectively, $\tilde{\mathbf{H}} = [\mathbf{h}(\delta, f_s),\ \mathbf{h}(-\delta, f_s)]$ with $\mathbf{h}(f, f_s) = [1,\ e^{j2\pi f/f_s},\ ...,\ e^{j2\pi(N-1)f/f_s}]^T$ and $\tilde{\mathbf{z}}_l = [a_1 a_2 e^{-j2\pi\phi_l},\ a_1 a_2 e^{j2\pi\phi_l}]^T$.

Let us briefly analyze the noise power of the low-frequency differential signal sampled in the RIPS-sq. The sampled aggregated noise in (4) can be written explicitly as

$$\tilde{v}_l[n] = u_l[n]v_l^*[n] + u_l^*[n]v_l[n] + v_l[n]v_l^*[n], \tag{5}$$

where $u_l[n] = \sum_{k=1}^{2} a_k e^{j2\pi(f_k - f_o)n/f_s - j2\pi\varphi_{k,l}}$. Recall that $v_l[n]$ is the normally distributed random variable with the mean of zero and the variance of σ_l^2. Therefore, the variance of $\tilde{v}_l[n]$ is given as

$$\mathrm{var}[\tilde{v}_l[n]] = \sigma_l^4 + 2\sigma_l^2 u_l[n]u_l^*[n], \tag{6}$$

which is greater than σ_l^2. Hence, the noise power is increased from a squaring operation in the RIPS-sq. To avoid the performance loss due to the increase in the noise power, we propose the RIPS-u that samples the raw-received signal at the low-sampling rate in the following subsection.

B. The RIPS-u

As shown at the upper part of Fig. 2, our proposing receiver passes the downconverted received signal $r_l(t)$ through a BPF and directly samples at the rate f_u. Collecting N samples and forming a column vector $\mathbf{r}_l$, we obtain

$$\mathbf{r}_l = \mathbf{H}\mathbf{z}_l + \mathbf{v}_l, \tag{7}$$

where $\mathbf{r}_l$ and $\mathbf{v}_l$ are the sampled vectors of $r_l(t)$ and $v_l(t)$, respectively, $\mathbf{z}_l = [a_1 e^{-j2\pi\varphi_{1,l}},\ a_2 e^{-j2\pi\varphi_{2,l}}]^T$, and $\mathbf{H} =$

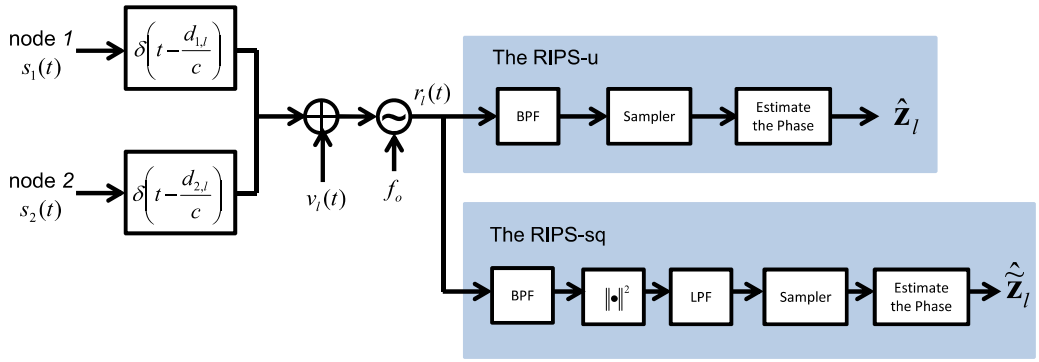

Fig. 2. The block diagram of the RIPS-u and the RIPS-sq.

$[\mathbf{h}(f_1 - f_o, f_u)\ \mathbf{h}(f_2 - f_o, f_u)]$. Note that the original phase term in $\mathbf{z}_l$ is independent of f_o and f_u. When $f_u < 2(f_1 - f_o)$, the signal is undersampled, and the frequency $f_k - f_o$ is aliased to $\mathrm{mod}(\mathrm{f_k} - \mathrm{f_o}, \mathrm{f_u})$, where $\mathrm{mod}(\mathrm{a}, \mathrm{b}) = \mathrm{a} - \lfloor \mathrm{a/b} \rfloor$ with $\lfloor \cdot \rfloor$ denotes rounding down towards zero. The extreme case is when two aliased frequencies are equal to each other, which happens when $\mathrm{mod}(\delta, \mathrm{f_u}) = 0$. However, as long as two aliased frequencies are well separated, the accurate phase estimates can still be achieved.

III. The Estimation of the Q-range

As shown in [13], the Q-range estimator for the RIPS-sq contains the approximation error $\eta = \delta/(2g)(d_{1,1} - d_{1,2} + d_{2,1} - d_{2,2})$. In this section, we present the Q-range estimator for the RIPS-u, which is free of approximation. Assuming the receiver knows values of f_1 and f_2, we can estimate $\mathbf{z}_l$ using a least-squares (LS) estimator as

$$\hat{\mathbf{z}}_l = \mathbf{H}^{\dagger}\mathbf{r}_l, \tag{8}$$

where $(\cdot)^{\dagger}$ denotes the pseudo-inverse. The phase vector $\mathbf{z}_l$ contains the distance metric as well as nuisance parameters such as t_k and θ_k. To cancel out these unwanted terms, consider the following expressions:

$$\begin{aligned} \alpha_1 =& \mathbf{z}_1^*[1]\mathbf{z}_2[1] = a_1^2 e^{j2\pi f_1 \frac{d_{1,1}-d_{1,2}}{c}}, \\ \alpha_2 =& \mathbf{z}_1[2]\mathbf{z}_2^*[2] = a_2^2 e^{-j2\pi f_2 \frac{d_{2,1}-d_{2,2}}{c}}, \end{aligned} \tag{9}$$

where $(\cdot)^*$ and $\mathbf{z}[i]$ denote the complex conjugation and the ith element of the vector $\mathbf{z}$, respectively. Note that unknown parameters t_k and θ_k are absent in (9), and only the range information is left in their phase. Unwrapping the phase of (9) may contain unknown integers unless $|d_{1,1} - d_{1,2}| < c/(2f_1)$ and $|d_{2,1} - d_{2,2}| < c/(2f_2)$. Assuming such conditions are satisfied, the Q-range estimator of the RIPS-u is given as

$$\hat{q}^{(u)} = \frac{c}{2\pi}\left\{\frac{1}{f_1}\arg(\hat{\alpha}_1) + \frac{1}{f_2}\arg(\hat{\alpha}_2)\right\}, \tag{10}$$

where the Q-range is defined as $q = d_{1,1} - d_{1,2} - d_{2,1} + d_{2,2}$. Following remarks are in order:

Remark 1: The RIPS-u samples the downconverted signal instead of the squared signal. Therefore, it has lower noise power than the RIPS-sq, which leads to the better performance.

Remark 2: The conditions imposed on the RIPS-u to assume that integers are zero in (10) are more strict than that of the RIPS-sq, which is $q < c/(2g)$. Furthermore, integers have to be solved when ranges are beyond the bounds for either RIPS's. In [13], the RIPS-sq employs multiple transmissions at different frequencies to obtain a set of Diophantine equations and to resolve integers. Also based on the multiple transmissions, the maximum likelihood (ML) approach [21] and the Chinese remainder theorem (CRT) based approach [22] are also proposed to resolve the integers in the RIPS-sq.

These methods can also be applied to the RIPS-u by switching the transmission frequencies between two transmitters. The sampled received signal is modeled as in (7) with $\mathbf{z}_l$ replaced with $\mathbf{y}_l = [a_2 e^{j2\pi\theta_2} e^{-j2\pi f_1(d_{2,l}+t_2)},\ a_1 e^{j2\pi\theta_1} e^{-j2\pi f_2(d_{1,l}+t_1)}]^T$. Similarly to (9), let us define $\beta_1 = \mathbf{y}_1^*[1]\mathbf{y}_2[1]$ and $\beta_2 = \mathbf{y}_1[2]\mathbf{y}_2^*[2]$. Then, two Q-range estimates w.r.t. f_k for $k = 1, 2$ can be achieved as

$$\hat{q}_k^{(u)} = \frac{c}{2\pi f_k}\arg(\hat{\alpha}_k\hat{\beta}_k^*) + \frac{c}{f_k}\bar{z}_k, \tag{11}$$

where $\bar{z}_k$ is the unknown integer. Now, the resolvable range is defined by $q < c/(2f_k)$, which is similar to that of the RIPS-sq since $f_k \approx g$ for $k = 1, 2$. In the case when the range may exceed these bounds, integers can be resolved using already available methods [21], [22] with appropriate designing of frequencies f_1 and f_2.

Remark 3: As shown in (7), the phase is independent of the sampling frequency f_u, and the RIPS-u can work with the undersampled signal as long as aliased frequencies are well separated. Hence, f_u can even be $f_u < \delta$. Moreover, note that the size of the approximation error η in the RIPS-sq is proportional to the ratio $\delta/(2g)$. Therefore, to keep η small, δ has to be sufficiently small compared to g in the RIPS-sq. On the other hand, since the RIPS-u is free of such an approximation, the choice of δ is not as restricted as the RIPS-sq. Therefore, the RIPS-u has more flexibility in its choice of parameters

compared to the RIPS-sq.

IV. Simulation Results

The performance of the RIPS-u is evaluated through Monte-Carlo simulations using MATLAB. Unless otherwise noted, frequencies are set at $f_2 = 10$ MHz, $\delta = 1.2$ kHz, $f_1 = f_2 + \delta$, $f_o = 9$ MHz, and the signal length is fixed at 25 millisecond (ms). The transmitted power is fixed to $a_k = 1$ for $k = 1, 2$, and $\sigma_l = \sigma$ for $l = 1, 2$. The SNR is defined as SNR = $1/\sigma^2$. Let us first examine how the sampling rate affects the performance of the RIPS-u. At each iteration, four nodes are randomly deployed in 10×10 meters squared area, and the Q-range is estimated with the RIPS-u. Under this setup, integer ambiguity can be avoided, and one transmission is sufficient to achieve the accurate Q-range estimate. Fixing the SNR at 20 dB, the sampling frequency f_u is varied from 100 Hz to 10 kHz. The RMSE of the Q-range estimates vs. f_u is shown in Fig. 3. The performance improves with increasing f_u since the number of samples increases as f_u increases with fixed signal length. Since $f_u < (f_2 - f_o) = 1$ MHz, frequencies are aliased. Yet, the figure shows that the range is accurately estimated. Also, the RIPS-u can achieve a submeter accuracy even when $f_u < \delta$.

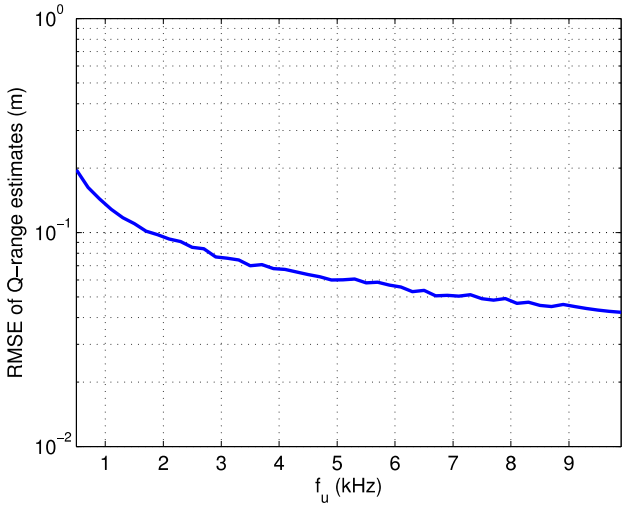

Fig. 3. The RMSE of the Q-range estimate of the RIPS-u vs. f_u.

To compare the performance of the RIPS-u and the RIPS-sq, we employ anchor nodes and estimate the location of the target node. Four anchor nodes A, B, C, and D are placed at the corner of the 10×10 meters squared area, where the position of node A is set as the origin, and the target node is randomly placed within this squared area at each iteration. The sampling frequency is fixed as $f_u = f_s = 4.8$ kHz. With these parameters, the approximation error in the Q-range estimator of the RIPS-sq is less than 0.002 meters. Since $f_u < 2(f_k - f_o)$, the frequencies of the downconverted signal in the RIPS-u are aliased as the signal is undersampled. Aliased frequencies are $\mathrm{mod}(\mathrm{f_1} - \mathrm{f_o}, \mathrm{f_u}) = 2.8$ kHz and $\mathrm{mod}(\mathrm{f_2} - \mathrm{f_o}, \mathrm{f_u}) = 1.6$ kHz, which are separated enough to facilitate the accurate phase estimation.

Let us denote the Q-range as $q(A, B, C, D) = d_{A,C} - d_{A,D} - d_{B,C} + d_{B,D}$. The performance of the Q-range estimation is evaluated by obtaining three Q-ranges $q(X, C, B, A)$, $q(X, B, C, A)$, and $q(X, B, D, A)$ (X denotes the target node). Recall that the receivers have to be synchronized. Since the synchronization between the target node and the anchor nodes is difficult to achieve, the target node is fixed as a transmitter. The RMSE of the Q-range estimates vs. the SNR over 2000 iterations is shown in Fig. 4. At each iteration, three Q-range estimates are obtained. In the simulation, there is approximately 3 dB gain in the performance of RIPS-u from the RIPS-sq because the RIPS-u has the lower noise power compared to the RIPS-sq. The error floor in the RIPS-sq in high SNR region is due to the approximated term.

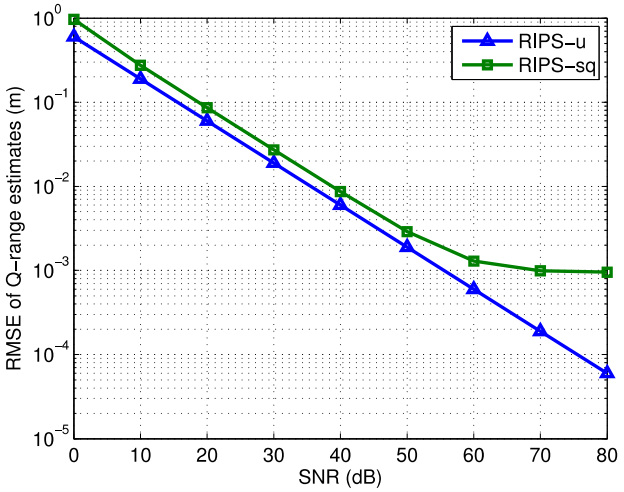

Fig. 4. The RMSE of the Q-range estimate vs. the SNR.

The localization based on the Q-range measurements is generally complicated since the Q-range involves four different distances. The iterative approaches such as the genetic algorithm are used in [13], [23], and the hyperbolic positioning method is proposed in [24]. The iterative approach takes time for a solution to converge, and the hyperbolic algorithm may result in ambiguous solutions depending on node locations. When the Q-range involves only one target node and rest are the anchor nodes at known locations, the range-difference (RD) can be obtained from the Q-range [17]. For instance, from the Q-range $q(X, A, B, C)$, the RD between the target node X and two anchors A and B can be obtained as

$$d_{X,B} - d_{X,C} = q(X, A, B, C) + d_{A,B} - d_{A,C}, \qquad (12)$$

where $d_{A,B}$ and $d_{A,C}$ can be precalculated based on the known locations of anchor nodes. The RD-based localization algorithms are already available in [25], [26].

Since three Q-ranges estimated in the previous subsection involve one target node, we can achieve the estimates of three RDs: $d_{B,X} - d_{A,X}$, $d_{C,X} - d_{A,X}$ and $d_{D,X} - d_{A,X}$. Then, the RD-based localization in [25] is employed to estimate the location of the target node X. The RMSE of the location estimates of the RIPS-u and the RIPS-sq vs. the SNR are shown in Fig. 5. As expected from the performance of the Q-range estimates plotted in Fig. 4, there is a slight performance gain for the RIPS-u over the RIPS-sq. Both the RIPS-u and the RIPS-sq reach a submeter accuracy when SNR > 10 dB.

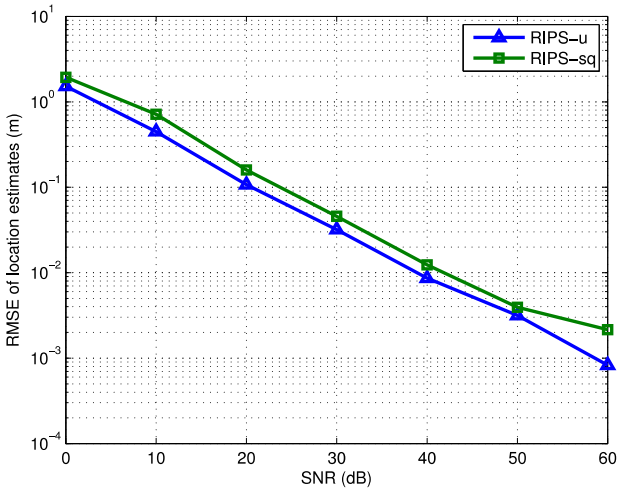

Fig. 5. The RMSE of the location estimate vs. the SNR.

V. Conclusions

In this paper, we proposed the RIPS receiver (RIPS-u) that samples the downconverted signal. By avoiding the squaring operation, the noise power in the RIPS-u is less than that of the RIPS using the square-law device (RIPS-sq). The RIPS-u achieves the Q-range estimates without the approximation since it can distinguish tones coming from two transmitters. Furthermore, we show that the accurate phase estimates can be still achieved even if the downconverted signal is undersampled. Therefore, the RIPS-u has more freedom in its parameter design compared to the RIPS-sq. The performance of the RIPS-u is evaluated by the MATLAB simulations, which confirm that the RIPS-u performances better than the RIPS-sq.

References

[1] I. Akyildiz, W. Su, Y. Sankarasubramaniam, and E. Cayirci, "A survey on sensor networks," *IEEE Commun. Mag.*, vol. 40, no. 8, pp. 102–114, Aug. 2002.

[2] N. Patwari, J. Ash, S. Kyperountas, A. Hero, R. Moses, and N. Correal, "Locating the nodes: cooperative localization in wireless sensor networks," *IEEE Signal Process. Mag.*, vol. 22, no. 4, pp. 54–69, Jul. 2005.

[3] G. Sun, J. Chen, W. Guo, and K. Liu, "Signal processing techniques in network-aided positioning: a survey of state-of-the-art positioning designs," *IEEE Signal Process. Mag.*, vol. 22, no. 4, pp. 12–23, Jul. 2005.

[4] T. He, C. Huang, B. M. Blum, J. A. Stankovic, and T. Abdelzaher, "Range-free localization schemes for large scale sensor networks," in *Proc. ACM MobiCom*, San Diego, CA, Sep. 2003, pp. 81–95.

[5] N. Bulusu, J. Heidemann, and D. Estrin, "GPS-less low-cost outdoor localization for very small devices," *IEEE Personal Commun. Mag.*, vol. 7, no. 5, pp. 28–34, Oct. 2000.

[6] P. Bahl and V. N. Padmanabhan, "RADAR: an in-building RF-based user location and tracking system," in *Proc. IEEE INFOCOM*, Tel Aviv, Mar. 2000, pp. 775–784.

[7] ——, "Enhancements to the RADAR user location and tracking system," Microsoft Research, Tech. Rep., 2000.

[8] X. Cheng, A. Thaeler, G. Xue, and D. Chen, "TPS: a time-based positioning scheme for outdoor wireless sensor networks," in *Proc. IEEE INFOCOM*, vol. 4, Hon Kong, China, Mar. 2004, pp. 2685–2696.

[9] Y. Wang, X. Ma, and G. Leus, "Robust time-based localization for asynchronous networks," *IEEE Trans. Signal Process.*, vol. 59, no. 9, pp. 4397–4410, Sep. 2011.

[10] S. Gezici, Z. Tian, G. Giannakis, H. Kobayashi, A. Molisch, H. Poor, and Z. Sahinoglu, "Localization via ultra-wideband radios: a look at positioning aspects for future sensor networks," *IEEE Signal Process. Mag.*, vol. 22, no. 4, pp. 70–84, Jul. 2005.

[11] T. Janson, C. Schindelhauer, and J. Wendeberg, "Self-localization application for iphone using only ambient sound signals," in *Proc. IEEE IPIN*, Zurich, Switzerland, Sep. 2010, pp. 1–10.

[12] C. Peng, G. Shen, Y. Zhang, Y. Li, and K. Tan, "Beepbeep: a high accuracy acoustic ranging system using COTS mobile devices," in *Proc. ACM SenSys*, Sydney, Australia, Nov. 2007, pp. 1–14.

[13] M. Maróti, B. Kusý, G. Balogh, P. Völgyesi, A. Nádas, K. Molnár, S. Dóra, and A. Lédeczi, "Radio interferometric geolocation," in *Proc. ACM SenSys*, San Diego, CA, Nov. 2005, pp. 1–12.

[14] B. J. Dil and P. J. M. Havinga, "A feasibility study of RIP using 2.4 GHz 802.15.4 radios," in *Proc. IEEE MASS*, San Francisco, CA, Nov. 2010, pp. 690–696.

[15] ——, "Stochastic radio interferometric positioning in the 2.4 GHz range," in *Proc. ACM SenSys*, Seattle, WA, Nov. 2011, pp. 108–120.

[16] H.-l. Chang, J.-b. Tian, T.-T. Lai, H.-H. Chu, and P. Huang, "Spinning beacons for precise indoor localization," in *Proc. ACM SenSys*, Raleigh, NC, Nov. 2008, pp. 127–140.

[17] B. Kusý, G. Balogh, J. Sallai, A. Lédeczi, and M. Maróti, "InTrack: high precision tracking of mobile sensor nodes," in *Proc. EWSN*, Delft, The Netherlands, Jul. 2007, pp. 51–66.

[18] B. Kusý, J. Sallai, G. Balogh, and A. Lédeczi, "Radio interferometric tracking of mobile wireless nodes," in *Proc. ACM MobiSys*, San Juan, Puerto Rico, Jun. 2007, pp. 139–151.

[19] Y. Wang, M. Shinotsuka, X. Ma, and M. Tao, "Design an asynchronous radio interferometric positioning system using dual-tone signaling," in *Proc. IEEE WCNC*, Shanghai, China, Apr. 2013, pp. 2294 – 2298.

[20] W. Zhang, Q. Yin, X. Feng, and W. Wang, "Distributed TDoA estimation for wireless sensor networks based on frequency-hopping in multipath environment," in *Proc. IEEE VTC*, Taipei, Taiwan, May 2010, pp. 1–5.

[21] W. Li, X. Wang, and B. Moran, "Resolving RIPS measurement ambiguity in maximum likelihood estimation," in *Proc. FUSION*, Chicago, IL, Jul. 2011, pp. 1–7.

[22] C. Wang, Q. Yin, and W. Wang, "An efficient ranging method based on Chinese remainder theorem for RIPS measurement," *Science China Information Sciences*, vol. 53, no. 6, pp. 1233–1241, 2010.

[23] N. Patwari and A. O. Hero III, "Indirect radio interferometric localization via pairwise distances," in *Proc. EmNets*, Cambridge, MA, May 2006.

[24] X. Wang, B. Moran, and M. Brazil, "Hyperbolic positioning using RIPS measurements for wireless sensor networks," in *Proc. IEEE ICON*, Adelaide, SA, Australia, Nov. 2007, pp. 425–430.

[25] P. Stoica and J. Li, "Lecture notes - source localization from range-difference measurements," *IEEE Signal Process. Mag.*, vol. 23, no. 6, pp. 63–66, Nov. 2006.

[26] Y. Wang and G. Leus, "Reference-free time-based localization for an asynchronous target," *EURASIP J. Advances in Signal Processing*, 2012:19, Jan. 2012, doi:10.1186/1687-6180-2012-19.